

Published in final edited form as:

Neurobiol Aging. 2007 March ; 28(3): 459–476.

Adult age differences in the functional neuroanatomy of visual attention: A combined fMRI and DTI study

David J. Madden^{a,b,*}, Julia Spaniol^{a,b}, Wythe L. Whiting^c, Barbara Bucur^a, James M. Provenzale^d, Roberto Cabeza^{a,e}, Leonard E. White^{a,f}, and Scott A. Huettel^{a,b,g}

a Center for the Study of Aging and Human Development, Duke University Medical Center, Box 2980, Durham, NC 27710, USA

b Department of Psychiatry and Behavioral Sciences, Duke University Medical Center, NC, USA

c Department of Psychology, Washington and Lee University, Lexington, VA 24450, USA

d Department of Radiology, Duke University Medical Center, NC, USA

e Center for Cognitive Neuroscience, Duke University, Durham, NC 27708, USA

f Department of Community and Family Medicine, Duke University Medical Center, NC, USA

g Brain Imaging and Analysis Center, Duke University Medical Center, NC, USA

Abstract

We combined measures from event-related functional magnetic resonance imaging (fMRI), diffusion tensor imaging (DTI), and cognitive performance (visual search response time) to test the hypotheses that differences between younger and older adults in top-down (goal-directed) attention would be related to cortical activation, and that white matter integrity as measured by DTI (fractional anisotropy, FA) would be a mediator of this age-related effect. Activation in frontal and parietal cortical regions was overall greater for older adults than for younger adults. The relation between activation and search performance supported the hypothesis of age differences in top-down attention. When the task involved top-down control (increased target predictability), performance was associated with frontoparietal activation for older adults, but with occipital (fusiform) activation for younger adults. White matter integrity (FA) exhibited an age-related decline that was more pronounced for anterior brain regions than for posterior regions, but white matter integrity did not specifically mediate the age-related increase in activation of the frontoparietal attentional network.

Keywords

Aging; Neuroimaging; White matter; Brain activation; Fractional anisotropy; Region of interest; Top-down processing; Visual search; Perception; Cognition; Response time

1. Introduction

Visual search and identification tasks engage multiple forms of attentional processing, including top-down (endogenous, cognitively driven) and bottom-up (exogenous, stimulus driven) components. The goal of both top-down and bottom-up processing is the guidance of attention to the search target [57,78]. Behavioral studies of age-related cognitive change have reported a decline in attentional functioning in tasks involving visual search and target identification, especially when attention must be divided among multiple display items or input channels [38,44]. Some degree of this age-related decline is a consequence of bottom-up

* Corresponding author. Tel.: +1 919 660 7537; fax: +1 919 684 8569. E-mail address: djm@geri.duke.edu (D.J. Madden).

deficits in the sensory and neural systems supporting the transmission of the visual signal [65,66,68]. Behavioral studies, however, have also identified some tasks in which there is an additional age-related decline in top-down attentional selection [16,73], which may in turn represent a broader deficit in the executive control processes of coordinating, planning, and updating currently available information [71,75,76].

Current models of visuospatial attention, based on functional neuroimaging investigations of healthy younger adults, suggest that attentional processes are mediated by a widely distributed neural network, with critical components located in prefrontal, deep gray matter, and parietal regions [12,18,28,31,77]. There is in addition some differentiation within this frontoparietal network, comprising temporoparietal and inferior frontal cortex in the case of bottom-up attention, and dorsal parietal and superior frontal cortex in the case of top-down attention [13,26,56,79]. The general theme of the neuroimaging results is that both frontal and parietal regions are sources of top-down attentional signals that modulate target detection activity in visual cortical regions, by raising the baseline activity for an attended object, counteracting the suppressive effects of surrounding distractors, and limiting the number of potential object representations [1,14,28,67].

Neuroimaging studies of older adults have reported an extensive and complex pattern of age-related change in brain structure and function, including visual attention [9,58]. The results suggest that age-related decline occurs in the task-related activation of visual sensory cortex, consistent with the behavioral evidence for age-related decline in the efficiency of bottom-up processing [40,58]. In some tasks this decline is also accompanied by increased activation of other components of the frontoparietal attentional network, which has been interpreted as a compensatory recruitment of cortical regions outside the task-relevant pathway [8,20]. Most often, the regions associated with increased activation for older adults have included dorsolateral prefrontal cortex [8,21,37,45,48], although age-related increases in the activation of deep gray matter structures [42] and parietal cortex [8,21,48] have also been observed.

Functional neuroimaging investigations of cognitive aging have been concerned primarily with the characterization and localization of age-related change in cortical function, that is, measures of cerebral metabolism and blood flow obtained from positron emission tomography (PET) and functional magnetic resonance imaging (fMRI). The cortical networks mediating cognitive function establish connectivity through white matter pathways, however, and localized changes in cortical activation within the attentional network (e.g., in the frontal lobes) may result from white matter changes at various points in the network [22,61,70].

Diffusion tensor imaging (DTI) provides information about the properties of white matter, by measuring both the rate and directionality of the displacement distribution of water molecules across tissue components [4,32]. In DTI, one measure of white matter integrity is fractional anisotropy (FA), the degree to which water molecules diffuse in a single direction, which in turn is affected by axonal restrictions and myelin content. Fractional anisotropy tends to decrease as a function of increasing age, even in the absence of significant disease, suggesting a corresponding decline in the structural integrity of white matter with age that could compromise axonal conduction and the efficiency of information transfer among distributed cortical networks [46,55]. Age-related decline in FA is typically more pronounced for anterior brain regions than for more posterior regions [24,54,62]. Independently of age, decreased white matter integrity is associated with lower performance on cognitive tasks [47], and this relation between white matter integrity and cognitive performance may in addition be altered as a function of age, in ways that are as yet not clear. The particular brain regions, for example, that exhibit an association between white matter integrity and cognitive performance may vary with age [41]. The disconnection of task-relevant cortical circuits by decreased white matter

integrity has been proposed as a general mechanism of age-related decline in cognitive performance [2,51,52].

To date, however, we know of no published report in which DTI and fMRI measures have been combined, within participants, in the assessment of age-related change in cognitive function. The primary goal of this study was to take this first step, by conducting this combined assessment in the investigation of age-related changes in visual attention. We tested the hypothesis that age-related changes in attentional functioning would be related to cortical activation as measured by event-related fMRI, and that this relation, in turn, would be mediated by white matter integrity as measured by DTI.

We were interested specifically in the use of top-down attention during visual search. Previous neuroimaging studies of age differences in visual search using multi-item displays [36,37] suggest that activation of visual processing (occipitotemporal) regions is greater for younger adults, whereas older adults exhibit relatively greater activation of the frontoparietal network. These previous studies, however, have not distinguished between top-down and bottom-up processing. Similarly, where age-related effects in top-down attentional control have been isolated, the experiments have used single-item displays that do not require the identification of a target item among distractors [42,48]. We therefore used a multi-item search task in which we could isolate top-down attentional effects, by comparing blocks of trials in which the probability of a target-defining feature (color) is either relatively low (neutral condition) or relatively high (guided condition) [39,43]. In addition, we adjusted the duration of the search displays between the age groups (while keeping the overall duration of visual stimulation constant), so that the influence of the age-related decline in bottom-up processing (i.e., occipitotemporal activation) would be less pronounced. Finally, with the aim of identifying network-dependent effects, we adopted a region of interest (ROI) approach in which we selected sets of gray matter ROIs likely to be critically involved in various aspects of visual search performance: frontal and parietal regions related to attentional and oculomotor control, deep gray matter regions related to sensory-motor integration and response initiation, and occipital regions related to visual sensory processing [12,18,28,31,77]. We generated white matter ROIs that target fiber systems coursing to and projecting from these gray matter regions.

We hypothesized that an age-related increase would occur in the magnitude of fMRI activation of the frontoparietal network [8,20], and that this age difference would in turn be relatively greater in the guided condition, due to the top-down attentional control elicited by the higher level of target predictability. An age-related increase in the activation of deep gray matter regions has been associated with the type of motor responses required by this search task [42], and we predicted this type of age difference in the present task. In contrast, an age-related decline typically occurs in the activation of visual cortical regions [7,36,37], but our adjustment of display duration in this experiment would be expected to reduce this age effect. Critically, we predicted that the relation between the measures of neural activation and behavioral performance would change as a function of adult age. We reasoned that if an age-related increase in frontoparietal activation does occur, then this activation will be more highly correlated with search performance for older adults than for younger adults, and that younger adults would instead be more likely to exhibit a correlation between performance and activation in visual cortical regions [34,37].

With regard to DTI, we predicted that an age-related decline in white matter integrity (as indexed by FA) would be evident, and that this decline would be more pronounced for anterior brain regions than for more posterior ones, as reported previously [24,54,62]. If, in addition, this age-related decline in white matter integrity is a mechanism of age-related neurocognitive change, then regression analyses should reveal that FA is related to age differences in fMRI activation. More specifically, from the perspective of a disconnection theory [2,51,52], we

would expect that FA would correlate with fMRI activation and, further, be a mediator of the relation between fMRI activation and visual search performance. Accordingly, the statistical control of individual differences in FA should lead to a decrease in the relation between activation and performance, especially within the frontoparietal network, and this mediating role of FA should be more clearly evident for older adults than for younger adults. Thus, our overall goal was to establish whether age-related change in cortical activation was associated specifically with top-down guidance during visual search, and to determine whether a disconnection model of white matter integrity could account for the age-related changes in activation.

2. Methods

2.1. Participants

The Institutional Review Board of the Duke University Medical Center approved the research procedures, and all participants gave written informed consent. The participants were 16 younger adults (8 women) between 19 and 28 years of age ($M = 23.4$ years) and 16 older adults (8 women) between 60 and 82 years of age ($M = 67.0$ years). All participants were right-handed, community-dwelling individuals. Younger adults and older adults did not differ significantly with regard to the number of years of education (younger adults' $M = 16.7$ years; older adults' $M = 17.5$ years). On a screening questionnaire, all participants reported being free of significant health problems such as atherosclerotic cardiovascular disease or hypertension. None of the participants reported taking medications known to affect cognitive functioning or cerebral blood flow. Participants scored a minimum of 27 points on the Mini Mental State Exam [17], a maximum of 9 on the Beck Depression Inventory [5], and had a minimum corrected binocular acuity for near point of 20/40. A neuroradiologist (one of the authors: J.M.P.) reviewed all participants' T₂-weighted structural brain images and judged them to be free of significant abnormalities such as atrophy, ventricular dilation, and hyperintense white matter lesions. Mean response time (RT) per item on a computerized digit-symbol test [64] was higher for older adults ($M = 1695$ ms) than for younger adults ($M = 1338$ ms), $t(30) = 4.8$, $p < 0.001$. Raw scores on the vocabulary subtest of the Wechsler Adult Intelligence Scale-Revised [74] did not differ significantly between the age groups (younger adults' $M = 65.3$; older adults' $M = 65.4$).

Participants performed the psychometric and screening tests in a separate session approximately 2 weeks before the scanning session. During the screening session participants also performed a version of the visual search task, and these data (combined with additional participants not participating in the fMRI testing) have been reported elsewhere [39]. All participants were also given an optometric examination prior to the scanning session, and a pair of lenses for the scanner goggles was ground for each participant based on his or her optometric prescription. Thus, each participant viewed the displays during scanning with his or her best corrected acuity.

2.2. Behavioral task

During fMRI scanning, participants performed a visual search task [39] in which, on each trial, they indicated via button press which of two target letters (E or R) was present in a display (Fig. 1). Display size was constant at four letters: each display contained three gray letters and one red letter (i.e., a color singleton) presented against a black background. The two task conditions, neutral and guided, differed in the likelihood with which the color singleton was also the E/R target. In the guided condition, the color singleton was likely to be the target (75% singleton targets and 25% nonsingleton targets), providing a basis for top-down attention. In the neutral condition, the color singleton had only chance probability of being the target (25% singleton targets and 75% nonsingleton targets). Across trials within each condition, the target was equally likely to be E or R for both singleton-target and nonsingleton-target trials. Thus,

the composition of each display, one red letter among three gray letters, was the same in each task condition, equating the bottom-up influences on performance. What differed across conditions was the predictability of the singleton-target correspondence, and differences in search performance across the conditions represent the top-down attentional effects of this predictability [39].

On each trial, the distractor letters were selected without replacement from the set, F, H, K, N, P, S, T, and X. The display items were arranged in a circle with six equidistant positions at 12, 2, 4, 6, 8, and 10 o'clock. Two diametrically opposite positions (e.g., 12 and 6 o'clock) were randomly chosen to be filled with a gray outline square that was approximately the size of a letter. The total duration of visual stimulation per trial was the same (2000 ms) for both age groups. As in the previous behavioral study using this task [39], we set the duration of the letter display at 1000 ms for younger participants and 1500 ms for older participants, to provide some compensation for age-related slowing of visual processing. Following the letter display, a mask of six pound signs (#) was presented at the six display locations, with a duration of 1000 ms for younger adults and 500 ms for older adults, yielding the 2000 ms total duration of visual events. Before the beginning of the next trial, a blank screen was presented for 500, 1000, or 1500 ms (each with 33% probability), and thus the average trial duration was 3 s.

Our goal was to examine age-related changes in top-down attention under conditions that minimized the age differences in bottom-up processing, and thus we provided older adults with additional time to view the letter displays. When display duration is held constant, task-related activation in visual cortical regions is typically lower for older adults than for younger adults, reflecting this age difference in bottom-up activation [7,36,37]. Using different display durations for younger and older adults raises the possibility that different search processes may be invoked in relation to display duration. Our interest here, however, was in the interactions between age group and task condition, which are independent of duration because the duration was identical for the neutral and guided conditions [7]. Although using the same duration for the two age groups may appear to be preferable, this solution is also imperfect. As a result of age-related slowing of information processing [38,63], older adults are obtaining less visual information per unit time than younger adults, so that what is ostensibly the same duration for the two age groups is in fact a shorter duration for older adults.

Participants were told that the most efficient way to perform the search task was to maintain fixation at the center of the display, although eye movements were not recorded, and saccades may have occurred during the display presentation. The neural activation associated with attending covertly to peripheral display locations overlaps substantially with the activation for executing a saccade [11,23,50], and we did not attempt to separate these processes in this context. Activation of the frontal eye field, for example, can occur in association with covert attentional shifts even when eye movement recording indicates no detectable change in eye position, whereas overt eye movement additionally leads to activation in primary visual (cuneus) and association visual cortical regions [14,19]. Top-down attention as measured here likely involves the combined effects of covert attentional orienting and the planning and execution of eye movements.

2.3. Imaging data acquisition

Scanning was conducted on a 1.5 T GE NVi SIGNA scanner with 41 mT/m gradients for fast image acquisition. Head motion was minimized with a vacuum-pack system that was molded to fit each participant. The following types of images were acquired, in the same order for all participants: sagittal localizer, T₁-weighted, T₂*-weighted (functional), spoiled gradient recalled (SPGR), DTI, and T₂-weighted. The high resolution SPGR sequence was obtained for assistance in defining anatomical ROIs.

The 2D T_1 -weighted images were 21 contiguous near-axial slices parallel to the anterior–posterior commissure (AC–PC) plane, 5 mm thick, with no interslice gap. The T_1 -weighted imaging used a gradient-echo sequence with TR/TE = 450/3.5 ms, flip angle = 90° , 256×256 image matrix, and in-plane resolution = 0.94 mm^2 .

The T_2^* -weighted functional images, sensitive to the blood–oxygen-level dependent (BOLD) signal, were acquired at the same slice locations as the 2D T_1 -weighted images (i.e., 21 contiguous slices parallel to AC–PC, each 5 mm thick). The functional scans used a spiral-out gradient-echo sequence, with TR/TE = 1500/40 ms, flip angle = 90° , 64×64 image matrix, and in-plane resolution = 3.75 mm^2 .

The DTI sequence included four signal averages, each acquiring 27 contiguous near-axial slices, parallel to AC–PC, 6 mm thick. Diffusion was measured in six directions, plus one image with no diffusion weighting [3]. The actual gradient strengths were adjusted for each direction to yield the desired b -value. Diffusion tensor imaging used a spin echo echo-planar sequence, with TR/TE = 12,000/82 ms, flip angle = 90° , $b = 1000 \text{ s/mm}^2$, 128×128 image matrix, and in-plane resolution = 1.88 mm^2 .

2.4. Event-related fMRI design and procedure

There were six functional imaging runs. We used an event-related design in which each scanner run contained both on-task and off-task (fixation) periods, with individual trials occurring at varying intervals during the task period. The first four images of each scanner run were discarded from functional analyses to allow longitudinal magnetization to stabilize. During the following two TRs, an instruction screen informed participants as to whether the upcoming trials were guided (“Target likely red”) or neutral (“Target unlikely red”). Following the instruction screen, each scanner run contained six task-fixation sequences, illustrated in Fig. 2. Each task period was 24 TRs (36 s), including 12 visual search trials of 2 TRs each, yielding 72 task trials per run. These 72 trials contained 54 singleton targets and 18 nonsingleton targets in the guided condition, and 18 singleton targets and 54 nonsingleton targets in the neutral condition. The pseudorandom variation in the intertrial interval (blank screen) among three values: 500, 1000, and 1500 ms (Fig. 1), provided a jitter in the display onset relative to the TR, thus increasing the temporal resolution of the estimated hemodynamic response (HDR). The 24 TR task period was followed by a central fixation cross, which did not require a response, presented for 13 TRs (19.5 s). A new task sequence began following this 13 TR period.

Neutral and guided task conditions were presented in alternating scanner runs (three for each task condition), which provided 162 singleton-target trials and 54 nonsingleton-target trials in the guided condition, and 54 singleton-target trials and 162 nonsingleton-target trials in the neutral condition. Two block orders were constructed that counterbalanced the serial position of individual trial blocks. Block order and response order (i.e., the assignment of target letters to response buttons) were counterbalanced across participants within each age group.

Within each block, the order of the target types (singleton target, nonsingleton target) was randomized, with the following constraints. In the neutral task condition, for both singleton-target and nonsingleton-target trials, the current trial was followed by a nonsingleton-target trial with a probability of approximately 67%, with the remaining instances being either singleton-target trials or fixation periods. Similarly, in the guided condition, the current trial was likely to be followed by a singleton target with a probability of approximately 67%. There were no more than nine successive targets of the same type (singleton target, nonsingleton target) in any block. The duration of each intertrial interval was randomized, with the constraint that within both neutral and guided task conditions, approximately 33% of the targets of each

target type (singleton target, nonsingleton target) were preceded by each of the three intertrial intervals (500, 1000, and 1500 ms).

The displays were projected from behind the scanner onto a liquid crystal display, and participants viewed the displays through goggles with attached mirrors. Participants responded by pressing two buttons on a fiber optic response box, using their left and right index fingers. Participants were encouraged to respond quickly and accurately. They first performed one block of 36 practice trials during collection of the anatomical images, which were not analyzed, followed by six blocks of 72 test trials corresponding to the six fMRI scanning runs.

2.5. fMRI data

Preprocessing of the fMRI data included correction for head motion and temporal order of slice acquisition within a TR, using SPM99 software (www.fil.ion.ucl.ac.uk/spm). Neither additional spatial smoothing nor normalization was performed, and subsequent analyses of the BOLD signal changes were performed using custom MATLAB (Math-works, Natick, MA) scripts, applied to anatomically defined ROIs for individual participants.

There were 13 ROIs for the fMRI data, which were drawn manually on individual slices of the near-axial T_1 images for each participant, using the sagittal and coronal views of the 3D SPGRs for additional guidance. Anatomical landmarks were identified by reference to an atlas with 1 mm axial MR slices [15]. Location and size of the regions are presented in Table 1, and examples of individual MR slices for the ROIs are presented in Fig. 3. This figure illustrates each ROI on one slice, although in practice each ROI spanned 2–11 slices (see Table 1). Similarly, Fig. 3 illustrates each ROI in one hemisphere, to allow inspection of the anatomy in the homologous hemisphere, but in practice all ROIs were drawn in both hemispheres.

We chose four sets of regions that, based on previous neuroimaging studies of visual attention [12,18,28,31,77], should capture the major contributions of top-down attentional control, visual processing, and response preparation: (i) frontal regions, including the rostral portion of the anterior cingulate, caudal portion of the anterior cingulate, middle frontal gyrus, and frontal eye field; (ii) deep gray matter structures, including the caudate, putamen, and thalamus; (iii) occipital regions, including the cuneus, fusiform gyrus, and lateral occipital gyri; (iv) parietal regions, including the angular gyrus, supramarginal gyrus, and superior parietal lobule.

In the frontal ROIs, the middle frontal gyrus was drawn using the superior frontal sulcus, inferior frontal sulcus, and (on superior slices) the precentral sulcus as major landmarks. The rostral anterior cingulate ROI included the portion of the cingulate gyrus anterior to the genu of the corpus callosum, whereas the caudal anterior cingulate ROI included more superior and posterior aspects of the anterior cingulate gyrus. The frontal eye field was identified as an area in the banks of the lateral precentral sulcus [35,59]. Although this premotor region likely resides in Brodmann area (BA) 6, just posterior to the location of the classical frontal eye field, BA 8 [6,29,33], the BA 6 region exhibits the highest concordance of activation across human neuroimaging studies of oculomotor control [23]. In the occipital ROIs, the cuneus was drawn using the calcarine and parieto-occipital sulci as the primary landmarks. The lateral occipital gyri were drawn to include those gyral structures between the cuneus and the anterior–lateral boundary of the occipital lobe. The fusiform (occipitotemporal) gyrus was drawn using the collateral sulcus as the medial boundary. In the parietal ROIs, the primary landmarks were the ascending segment of the superior temporal sulcus (for the angular gyrus) and the intra-parietal sulcus (for the superior parietal lobule). The supramarginal gyrus was drawn caudally to the postcentral gyrus, using the ascending ramus of the lateral fissure as a principal sulcal landmark.

A team of two trained operators outlined frontal and deep gray matter regions; another team of three operators outlined parietal and occipital regions. Operators within each team were

assigned equal numbers of image volumes from younger and older participants but were blinded to participant age. The spatial overlap between ROIs for these shared participants served as a measure of consistency among operators, expressed as the percentage of common voxels [10,42,49]. Before operators drew regions on nonshared participants, we determined that the percentage of spatially overlapping voxels on a set of shared images reached at least 80% for each team. The ROI size, in terms of number of voxels, was generally lower for older adults than for younger adults (Table 1), but the age difference was not statistically significant for any of the ROIs.

The T_1 images and ROIs were coregistered to the functional images using SPM99 software. Coregistered volumes were visually inspected and corrected as necessary. A low-pass filter was applied to the T_2^* images around the event frequency of 0.33 Hz to remove periodic effects of the task itself, independent of task conditions. To reduce variability in the time course data, we excluded from further analysis the TRs corresponding to incorrect responses [48].

2.6. DTI data

The DTI images were processed using custom MATLAB scripts that calculated the diffusion tensor eigenvalues ($D1$, $D2$, and $D3$) in each voxel. The FA values were calculated from Eq. (1):

$$FA = \frac{[(3/2)((D1 - Dav)^2 + (D2 - Dav)^2 + (D3 - Dav)^2)]^{1/2}}{DM}, \quad (1)$$

where $Dav = (D1 + D2 + D3)/3$ and $DM = (D1^2 + D2^2 + D3^2)^{1/2}$.

White matter ROIs were drawn directly on individual tensor image slices for each participant, following the methods used with the fMRI data (see Table 2). Due to the inherent distortion of the tensor images it was not possible to coregister them to the T_1 -weighted series, but the T_1 -weighted and SPGR images were used for additional guidance in drawing the white matter ROIs.

The eight white matter ROIs, illustrated in Fig. 4, were selected to target components of white matter pathways relevant for the gray matter ROIs, though (given the resolution available in the DTI images) not necessarily with a point-to-point correspondence with the gray matter ROIs. These included: (i) four relatively anterior regions, including the genu of the corpus callosum, frontal white matter just lateral to the genu (pericallosal frontal), white matter within the superior frontal gyrus, and the anterior limb of the internal capsule; (ii) four relatively posterior regions, including the splenium of the corpus callosum, medial occipital white matter (posterior visual), white matter associated with the fusiform gyrus, and parietal white matter. Before drawing the regions, operators set the maximum FA to a low value (0.30), so that all voxels with values greater than this criterion were saturated and appeared homogeneously as pure white. This procedure helped minimize the influence of voxels with higher FA values on the definition of the shape of the ROI. No thresholding was performed on the extraction of FA within the ROIs. A team of two operators drew the parietal region and a team of five operators drew the other seven ROIs. Prior to drawing ROIs independently, operators within each team attained at least 80% overlap of voxels.

The genu and splenium of the corpus callosum and the anterior limb of the internal capsule were clearly visible on the T_1 -weighted images, and thus standard anatomical land-marks were used to define these regions. The pericallosal frontal and superior frontal gyrus ROIs were defined on image slices containing the genu of the corpus callosum. The pericallosal ROI targeted the anterior centrum semiovale, where fibers of passage associated with dorsal

prefrontal cortical areas and related subcortical structures would be expected to course. This ROI was bounded by gray matter at the fundi of frontal sulci anteriorly and laterally (it did not sample subcortical white matter within frontal gyri), by the anterior horn of the lateral ventricles medially, and by insular cortex posteriorly. The superior frontal gyrus ROI was drawn generally on the same slices as the pericallosal ROI, comprising the white matter between the latter region and the gray matter of the superior frontal gyrus. The fusiform ROI was drawn on slices inferior to the thalamus, targeting the medially located white matter associated with the fusiform gyrus, with the parieto-occipital sulcus as its posterior boundary. The posterior visual ROI was defined in slices that contained the thalamus. This ROI targeted the medially located white matter associated with the cuneus and occipital gyri, with the parieto-occipital sulcus as its anterior boundary. The inferior limit of the parietal ROI was the most superior slice on which the ventricles were visible. This ROI was bounded anteriorly by extending an imaginary line parallel from the fundus of the central sulcus and posteriorly by the parieto-occipital sulcus. We sampled white matter within this area, avoiding the splenium of the corpus callosum. Tests of age group differences in the number of voxels per region yielded significant effects for the genu, $t(30) = 2.09$, $p < 0.05$, pericallosal frontal region, $t(30) = 2.77$, $p < 0.01$, superior frontal gyrus, $t(30) = 3.58$, $p < 0.001$, and the parietal region, $t(30) = 2.64$, $p < 0.01$, all of which exhibited an age-related decline in white matter ROI size (Table 2).

2.7. Magnitude and spatial extent of event-related activation

The time series for event-related effects were linearly detrended to remove drift effects across the task period. We calculated averaged voxelwise epochs for each combination of participant, condition (neutral versus guided), target type (singleton versus nonsingleton), and hemisphere (left versus right), using custom MATLAB tools. Each averaged epoch spanned 12 TRs (18 s), including the three image volumes preceding the trial onset and the nine volumes following trial onset. The average response on the first four volumes served as a pre-event baseline of activity during the task period. The percentage signal change, relative to this baseline, was calculated for each volume of the epoch.

We correlated the averaged time series for each voxel with an empirical reference waveform [27] that represented the time course of the average event-related HDR observed in the present study. Thresholding was performed using t statistics derived from the resulting correlation coefficients by creating separate spatial maps for voxels activated by each of the four combinations of task condition and target type. Voxels whose correlations with the reference waveform met a $p < 0.10$ threshold were included in each map. We adopted a relatively liberal threshold at this early stage (i.e., prior to the task condition analyses), because the goal was to eliminate only those voxels that were not active in some biologically plausible way. The four maps were then combined into a final map of voxels activated by any of the four combinations of condition and target type. This thresholding ensured that voxels without systematic responses to any of the trial events did not contribute noise to the average HDRs for each ROI.

To obtain the HDR curve we connected the average percentage change values of suprathreshold voxels as a function of TR; no curve fitting was performed. The dependent variable representing the magnitude of activation was the area under the HDR curve. We obtained this latter measure by obtaining the area under each pair of adjacent points on the HDR curve and summing the results. The area under the curve measure did not include deactivations (i.e., decreases in activation relative to the fixation baseline level).

We also determined the spatial extent of activation, by obtaining the percentage of voxels above threshold at $p < 0.05$ for each ROI, based on the t statistics for the correlation with the reference waveform.

2.8. Statistical analyses

Preliminary analyses of the magnitude of event-related activation (area under the HDR curve) indicated that there were few significant (or interpretable) effects of left versus right cerebral hemisphere. The independent variable of hemisphere was consequently dropped, and we present the results averaged over hemisphere. The independent variables in the event-related analyses were age group, task condition, and target type. All of the independent variables except age group were within-subjects. Top-down attentional effects were represented by significant changes in task performance and activation associated with the guided condition, relative to the neutral condition.

We divided the gray matter ROIs into four groups corresponding to their anatomy: frontal, deep gray matter, occipital, and parietal. To control for multicollinearity among the variables, and to protect against Type I error, we performed multivariate analysis of variance (MANOVA) for the HDR magnitude within each group of ROIs [69]. Univariate tests of the independent variables, for an individual ROI, were conducted only when the corresponding MANOVA effect (Wilks' Lambda) for the regional group was significant at $p < 0.05$.

Using a similar approach, we analyzed the eight white matter ROIs by two separate MANOVAs, one on the relatively anterior regions (genu, pericallosal frontal, superior frontal gyrus, and anterior limb of internal capsule), and one on the relatively posterior regions (splenium, posterior visual, fusiform, parietal). The dependent variable in this case was the average FA within each ROI, and univariate tests of the age group effect were conducted only when the MANOVA effect was significant.

3. Results

3.1. Visual search performance

Response time and error rate in the visual search task are presented in Table 3. Error rate was low and did not differ significantly as a function of age group (younger adults $M = 2\%$; older adults $M = 1\%$). In the analysis of RT for correct responses, we obtained the median RT for each participant in each combination of task condition and target type. Univariate analysis of variance (ANOVA) conducted on these RT data, with the between-subjects variable of age group and the within-subjects variables of condition and target type, yielded significant main effects for all three variables. The mean of the median RTs was higher for older adults ($M = 848$ ms) than for younger adults ($M = 654$ ms), $F(1, 30) = 50.51$, $p < 0.0001$, higher for the guided condition ($M = 757$ ms) than for the neutral condition ($M = 744$ ms), $F(1, 30) = 5.08$, $p < 0.05$, and higher for nonsingleton targets ($M = 808$ ms) than for singleton targets ($M = 694$ ms), $F(1, 30) = 103.0$, $p < 0.0001$. The interactions of age group \times target type, $F(1, 30) = 6.40$, $p < 0.05$, condition \times target type, $F(1, 30) = 156.85$, $p < 0.0001$, and age group \times condition \times target type, $F(1, 30) = 23.07$, $p < 0.0001$, were also significant.

To examine the interaction effects in the RT data, we analyzed the target type effect, defined as the percentage difference in RT between singleton and nonsingleton targets (Eq. (2)).

$$\text{Target type effect} = \left[\frac{\text{nonsingleton RT} - \text{singleton RT}}{\text{nonsingleton RT}} \right] \times 100 \quad (2)$$

Thus, the target type effect represents the relative difference in RT between singleton and nonsingleton targets, within each task condition, using the nonsingleton-target trials as a baseline.

In the guided condition, there was a substantial effect of target type that was significantly greater for older adults ($M = 24\%$) than for younger adults ($M = 17\%$), $F(1, 30) = 7.25$, $p <$

0.01. The corresponding measure in the neutral condition was smaller and comparable for the two age groups (younger adults' $M = 6\%$; older adults' $M = 5\%$), $F(1, 30) < 1.0$. These results represent a pattern in which, relative to the neutral condition, the guided condition led to both a decrease in RT for singleton targets and an increase in RT for nonsingleton targets. As a result, the difference between the two target types was more prominent in the guided condition than in the neutral condition. This pattern was in addition more pronounced for older adults than for younger adults.

3.2. Magnitude of activation

The significant statistical effects in the event-related analysis of the magnitude of activation are presented in Table 4, and the mean values (averaging left and right hemispheres) are displayed in Figs. 5 and 6. These analyses yielded two main findings. First, there was an age-related increase in activation within the frontoparietal network. The multivariate main effect of age group was significant for the frontal and parietal regions, which was the result of an age-related increase in activation in the frontal eye field, middle frontal gyrus, angular and supramarginal gyri, and superior parietal lobule. Second, activation was associated specifically with the use of top-down attention in the guided condition. The multivariate main effect of task condition was significant only for the parietal regions, as the result of greater activation for the guided condition than for the neutral condition, in the angular gyrus and superior parietal lobule.

Activation related to the singleton and nonsingleton targets also varied across the task conditions. The multivariate main effect of target type was significant within the deep gray matter and parietal regions, reflecting overall higher activation for nonsingleton targets than for singleton targets, in the thalamus and superior parietal lobule. This effect was modulated, however, by the multivariate interaction of condition \times target type, which was significant for all four sets of ROIs. The corresponding univariate interaction was significant for all of the frontal and parietal regions, for the thalamus within the deep gray matter regions, and for the cuneus and fusiform gyrus within the occipital regions. Simple effect tests conducted for each task condition demonstrated that, for each region associated with a significant univariate effect of target type, activation was higher for singleton targets than for nonsingleton targets in the neutral condition, whereas activation was higher for nonsingleton targets than for singleton targets in the guided condition.

3.3. Spatial extent of activation

As a measure of the spatial extent of task-related activation, we calculated the percentage of suprathreshold voxels within each ROI. Averaged across participants, the mean percentage of activated voxels within each combination of ROI, age group, and task condition ranged from 4 to 20% ($M = 9\%$). A regression analysis yielded a positive correlation between the spatial extent and activation magnitude values, $r = 0.31$, $p < 0.01$, indicating that increases in activation magnitude were generally accompanied by increases in spatial extent. In addition, when a variable was added to the regression model representing the change in the activation-spatial extent correlation as a function of age group (i.e., variables for activation and the age difference in activation as simultaneous predictors of spatial extent), the parameter estimate for the age effect was not significant. These spatial extent data are useful for ensuring that the age group and task condition effects in the activation magnitude data are not due to the effects of isolated voxels.

3.4. Correlation between activation and task performance

We examined the correlation between search performance (in terms of the target type effect; Eq. (2)) and the magnitude of event-related activation for individual ROIs, within each age group. In the guided condition, three ROIs exhibited a significant correlation between

activation on the singleton-target trials and the RT measure (see Fig. 7): for the frontal eye field, there was a significant activation–RT correlation for older adults, $r = 0.57$, $p < 0.02$, but not for younger adults. Similarly, for the superior parietal lobule, there was a significant correlation for older adults, $r = 0.66$, $p < 0.01$, but not for younger adults. For the fusiform gyrus, in contrast, there was a significant correlation between activation and RT for younger adults, $r = 0.52$, $p < 0.05$, but not for older adults. All three correlations were positive, indicating that increasing activation was associated with a larger effect of target type in RT. Regression analyses conducted for all participants combined indicated that the age group difference in the activation–RT correlations was significant for all three ROIs at $p < 0.05$.

On the nonsingleton-target trials in the guided condition, the activation–RT correlation for younger adults was significant for one region, the caudal portion of the anterior cingulate, $r = -0.52$, $p < 0.05$. The corresponding correlation was not significant for older adults, and a regression analysis of the two age groups combined indicated that the age difference in this correlation was not significant. In the neutral condition, activation on neither the singleton-target trials nor the nonsingleton-target trials was correlated with the target type effect.

3.5. Sustained activation

In this experiment, each fMRI imaging run contained six on-task/off-task sequences, and it is thus possible to estimate the average sustained activation during the task period, relative to the off-task (fixation) period. This estimate, though not entirely independent of the event-related effects, provides one measure of more general attentional processes that are common to the different trial types, such as maintaining task information in working memory and preparing to visually scan the display. Previous studies suggest that the initiation of a task period is accompanied by an abrupt increase in activation typically lasting several TRs, which then decreases to a more steady-state level throughout task performance [26,72]. We conducted preliminary analyses of the steady-state portion of these sustained effects, by modeling the area under the HDR curve for the final 18 TRs of each on-task period, using the final 6 TRs of the associated off-task (fixation) period as the baseline. Multivariate analyses revealed a significant age-related increase in this sustained activation for frontal regions, $F(4, 27) = 5.73$, $p < 0.01$, and parietal regions, $F(3, 28) = 4.22$, $p < 0.01$, but not for the deep gray matter or occipital regions. This age-related increase in sustained frontoparietal activation did not vary significantly as a function of neutral versus guided task condition.

Is the correlation between search performance and event-related activation in the guided condition, depicted in Fig. 7, a consequence of the age-related increase in sustained frontoparietal activation? To address this issue we conducted hierarchical regression analyses, for each of the three significant correlations illustrated in Fig. 7, entering the mean value of sustained activation in the relevant region of interest as the first predictor in the regression model, thus covarying the effect of sustained activation. When the older adults' sustained activation of the frontal eye field was entered first in the regression model, the event-related activation in the frontal eye field was no longer a significant predictor of the target type RT effect. When, however, the older adults' event-related activation in the superior parietal lobule was covaried for sustained activation in the superior parietal region, the event-related parietal activation remained a significant predictor of the target type effect, $F(1, 13) = 9.31$, $p < 0.01$. (The same pattern occurred if the covariate was the mean of the sustained activation in the frontal eye field and superior parietal regions.) Similarly, when the younger adults' event-related activation in the fusiform gyrus was covaried for the sustained fusiform activation, the event-related activation remained a significant predictor of the target type effect, $F(1, 13) = 9.91$, $p < 0.01$.

3.6. DTI fractional anisotropy

The mean FA values are presented, as a function of age group and region, in Fig. 8. The MANOVA of the anterior ROIs yielded a significant multivariate effect of age group, $F(4, 27) = 8.96, p < 0.0001$. Univariate effects of age group were significant for two regions, the pericallosal frontal region, $F(1, 30) = 18.65, p < 0.001$, and superior frontal gyrus, $F(1, 30) = 9.92, p < 0.01$, reflecting age-related decline in FA in each case. The multivariate effect of age group was not significant for the posterior regions.

In a series of regression analyses we investigated whether age differences in white matter integrity, as reflected in the FA values, were related to the age differences in fMRI activation. To reduce the likelihood of Type I error, we limited the regression analyses to those ROIs that had exhibited a significant age difference in either activation or FA. Two age-related effects were prominent in the fMRI activation data: the overall higher magnitude of activation in the frontoparietal ROIs for older adults, relative to younger adults (Figs. 5 and 6), and the age-related change in the activation–RT correlations (Fig. 7). To examine the relation between FA and the first age-related effect, we conducted bivariate correlations between FA and activation (averaged over task condition and target type) for each of the frontoparietal regions exhibiting a significant age difference in mean activation (frontal eye field, middle frontal gyrus, angular gyrus, supramarginal gyrus, and superior parietal lobule) and each of the white matter regions exhibiting a significant age difference in mean FA (pericallosal frontal, superior frontal gyrus). That is, within each age group, for those regions exhibiting an age difference, is there a significant relation between cortical activation and white matter integrity? This analysis, however, indicated that none of the correlations between activation and FA was significant for either age group.

Because the significant age-related changes in the activation–RT correlation (Fig. 7) were associated specifically with the singleton-target activation in the guided condition, in further analyses we limited the FA correlations to those trials. The relevant ROIs from the activation analyses were the frontal eye field, superior parietal lobule, and fusiform gyrus, and we again included the FA values for the pericallosal frontal and superior frontal ROIs. For the younger adults, there were no significant correlations between activation and FA. For the older adults, those individuals exhibiting higher activation in the superior parietal lobule also exhibited lower pericallosal frontal FA, $r = -0.49, p < 0.05$ (Fig. 9). To determine whether pericallosal frontal FA was a mediator of the relation between superior parietal lobule activation and RT, we repeated the regression model characterizing the activation–RT relation for older adults (Fig. 7), but included pericallosal frontal FA as a predictor of RT in a first step, prior to including superior parietal activation as a predictor. In this model, the FA variable was not significant as a predictor of the older adults' target type RT effect, but superior parietal activation remained significant as a predictor, when entered after pericallosal frontal FA, $F(1, 13) = 9.64, p < 0.01$.

4. Discussion

In this research we combined behavioral data from visual search performance, cortical activation from event-related fMRI, and white matter integrity from DTI, to investigate age-related changes in the functional neuroanatomy of visual attention. On the basis of previous findings, we predicted that activation in a frontoparietal network would be greater for older adults than for younger adults, especially when the task required top-down attentional control. We also expected that the regional pattern of correlation between cortical activation and search performance would differ between the age groups, involving the frontoparietal network in the case of older adults and visual (occipitotemporal) regions in the case of younger adults. Finally, as a test of a disconnection theory, we hypothesized that an age-related decline in white matter integrity (FA), especially in anterior brain regions, would be evident, and that we could characterize the FA changes as a mediator of the age-related changes in cortical activation.

Overall, our results lend support to some of these hypotheses, especially with regard to the age-related change in the relation between activation and performance, and to the age-related decline in FA. There was more limited support, however, for the role of FA as a mediator of the age differences in activation.

4.1. Visual search performance

The behavioral data (Table 3) support our previous observation that, in this type of search task, the use of top-down attentional control is preserved during healthy aging [39,43]. Although an age-related decline exists in some forms of attentional control [71,75,76], this decline is not absolute. In the present task, older adults' search performance was slower than that of younger adults, but both age groups exhibited evidence of top-down attentional control, and the older adults actually exhibited a greater reliance on top-down attention than younger adults. The critical finding in this regard is that the target type effect (i.e., percentage increase in RT for non-singleton targets, relative to singleton targets) was similar for the two age groups (5–6%) when there was a relatively low proportion of singleton-target trials (neutral condition), but was significantly greater for older adults (24%) than for younger adults (17%) when there was a higher proportion of singleton targets (guided condition). The small but reliable target type effect in the neutral condition suggests either that the color singleton captured attention automatically (i.e., a bottom-up effect) or that participants were using top-down attention to some extent during the neutral condition.

4.2. Event-related fMRI activation

In the event-related analyses of the magnitude of activation in response to individual trials, the dependent variable was the average area under the HDR of active voxels [48]. This measure was correlated positively, across task conditions, with the spatial extent of activation, and this correlation did not differ significantly between the age groups. The area under the HDR thus does not represent just the activity of isolated voxels. Analyses of the mean level of activation as a function of age group and task condition yielded two main findings (Figs. 5 and 6): an age-related increase in the activation of the frontoparietal network (independently of the task conditions) and an increase in the activation of parietal regions associated with the guided condition (independently of age group).

The age-related increase in frontoparietal activation is consistent with our initial hypothesis, but we had the additional prediction that this type of age effect would be more pronounced in the guided condition than in the neutral condition, which did not occur. Thus, the higher level of frontoparietal activation for older adults, relative to younger adults, is not due entirely to top-down attentional control and includes more general attentional processes common to the neutral and guided conditions. Because the duration of individual letter displays was 500 ms longer for older adults than for younger adults, and the central fixation cross was presented only during the off-task period, the frontoparietal activation may represent an increased degree of eye movement planning or number of saccades on the part of older adults [30,60].

The increased level of activation in the parietal regions, specifically the angular gyrus and superior parietal lobule, associated with the guided condition, is evidence for a top-down form of attentional guidance. To the degree that participants relied on the increased probability of the singleton-target correspondence in the guided condition, responses to individual displays would involve additional top-down control: the shift of attention to the singleton would be more deliberate, and the shift away from this display location (on nonsingleton-target trials) would be more difficult, requiring heightened spatial attention, facilitated by increased parietal activation. This result suggests a specifically top-down form of spatial attention mediated by the parietal lobe [13,14,56,79]. In terms of the mean level of activation, however, this top-down attentional effect was comparable for younger and older adults.

Two additional aspects of the activation magnitude analyses are relevant. First, the age-related increase in frontoparietal activation was not accompanied by the age-related decline in occipitotemporal activation that is typically observed when display duration is constant for the two age groups [7,36,37]. Although this is a null effect that may have occurred for a variety of reasons, the goal of providing a longer display duration for older adults was to equate visual cortical activation for younger and older adults, thus providing additional specificity in interpreting the age-related changes in activation outside of the visual cortical regions. Secondly, contrary to our initial expectation, there was no age-related change in the activation of deep gray matter regions. The response selection demands in this search task (i.e., pressing a key corresponding to the E/R target) were constant on each trial, and thus eliciting an age-related increase in deep gray matter activation may require a shift between motor responses as well as an attentional shift between display locations [42].

4.3. Correlation between activation and performance

A significant age difference in top-down attentional control was evident in the regression analyses of the correlation between activation and behavioral performance. In previous neuroimaging investigations of age differences in visual search, the bottom-up and top-down attentional effects were not separable [36,37]. Here we report new evidence for a specific age difference in the top-down component. The correlations between activation magnitude and the RT measure of search performance (target type effect) were associated specifically with the top-down component of attentional guidance (i.e., the guided condition). The activation-performance correlations involved the frontal eye field and superior parietal lobule for older adults and the fusiform gyrus for younger adults (Fig. 7). For both age groups, the correlations were positive, indicating that those individuals with greater activation in these regions exhibited a greater influence of attentional guidance on search performance. Within the guided condition, the correlations were more reliable for the singleton-target trials than for the nonsingleton-target trials, which likely reflects the greater number of singleton targets (162) than nonsingleton targets (54) in this condition [25]. Thus, in the guided condition, when the color singleton was more predictive of the search target, younger adults' performance was coupled with activation of a visual feature recognition region, whereas older adults' performance was more dependent on the frontal and parietal regions associated with the top-down maintenance of task goals, oculomotor control, and the spatial allocation of attention [1,18,28,31,77].

Analyses of the sustained activation throughout the on-task period, relative to the off-task period, demonstrated some differentiation of function within the frontoparietal network. For the older adults, the top-down attentional demands of the guided condition are not limited to event-related effects, but also (in the case of the frontal eye field) share variance with the sustained effects that were common to the neutral and guided conditions. Covarying sustained activation in the frontal eye field eliminated the older adults' correlation between event-related activation in this region and performance. In contrast, the older adults' event-related parietal activation in the guided condition, when covaried for sustained parietal activation, remained correlated significantly with search performance. This pattern may represent the enhanced preparation for visual scanning and target identification mediated by the frontal eye field throughout the task period. The top-down shift of attention either to or away from the singleton, on individual trials, however, is related more specifically to the superior parietal region [14, 28,79].

Older adults' increased reliance on frontoparietal mechanisms to support search performance may be a compensation for decline in the efficiency of bottom-up processes mediated by visual cortical regions [8,20]. Additional top-down attention, for example, may assist older adults by limiting the number of potential object representations, within an inherently noisier neural

signal [1,66]. Younger adults' performance in this search task may be mediated by visual cortical regions, with a minimum of attentional demands, whereas older adults' performance relies on a more widely distributed frontoparietal network supporting the maintenance of the relevant task set and behavioral goals. In the present experiment, however, both the accuracy of search performance and the magnitude of activation in visual cortical regions were comparable for the two age groups. The age difference in the pattern of correlations is thus not due entirely to a deficit in bottom-up processing, at least as reflected in the level of cortical activation.

4.4. White matter integrity from DTI

Two main findings emerged from the analyses of the FA values. First, as hypothesized, we replicated the previously reported pattern of the age-related decline in FA being more pronounced for anterior brain regions than for posterior regions [24,55,62]. Although mean FA was lower numerically for older adults than for younger adults in all regions, except the anterior limb of the internal capsule (Fig. 8), the multivariate effect of age group was significant only for the anterior regions. This age effect, in turn, was driven primarily by the age-related decline in FA for the white matter within the superior frontal gyrus and pericallosal frontal region. Thus, although aging likely leads to some degree of decline in white matter integrity throughout the brain, this decline appears to be more clearly evident within the frontal lobe.

Our second finding bears on the proposed role of age-related decline in white matter integrity as a mechanism of age-related change in cortical activation (and ultimately in cognitive performance). According to a disconnection hypothesis, age-related decline in white matter integrity, especially in prefrontal regions, disrupts the connectivity of the cortical networks mediating cognitive function [2,51,52]. When the fMRI activation on the singleton-target trials in the guided condition was examined separately, the correlation between activation in the superior parietal lobule and FA for the pericallosal frontal region was significant for older adults (Fig. 9): those older adults with relatively lower FA values exhibited relatively higher levels of activation, which is suggestive of a role for white matter integrity in the age-related increase in frontoparietal activation in the guided condition (Fig. 7). This apparent interaction between widely distributed components of the frontoparietal network is consistent with the existence of several white matter pathways, within the superior longitudinal fasciculus, linking prefrontal and parietal cortical regions [53]. When we examined the disconnection hypothesis more directly, however, by including FA as a predictor in the regression model relating the older adults' superior parietal activation to search performance, no effect of FA was evident. Thus, although we observed some relation between white matter integrity and activation for older adults (Fig. 9), white matter integrity was not a specific mediator as proposed by a disconnection model. Additional tests of a disconnection model are worth pursuing, however, especially with higher resolution DTI, permitting a more sensitive interrogation of white matter pathways and definition of their relation to gray matter regions.

5. Conclusion

The functional neuroanatomy of visual attention comprises both age-independent and age-related effects. Independently of adult age, posterior regions of the attentional network (angular gyrus and superior parietal lobule) are activated by top-down attention, when there is a high proportion of trials on which a salient visual feature (a color singleton) can be used to guide attention to a search target. Within this guided condition, on singleton-target trials, there is an age-related difference in the correlation between activation and performance (differentiation of singleton and nonsingleton targets), which appears to reflect top-down attentional control. Even under conditions that do not lead to a pronounced age-related decline in occipital activation, older adults place more emphasis than younger adults on the top-down attentional

mechanisms supported by the frontoparietal network. Age-related change also occurs in the integrity of the white matter regions related to this attentional network. Prefrontal regions exhibit relatively greater age-related decline in white matter integrity, and this decline is associated with greater fMRI activation for older adults, though not to the extent predicted by a disconnection model. Additional research combining fMRI, DTI, and behavioral performance will be valuable in determining the neural mechanisms of age-related cognitive change.

Acknowledgements

This research was supported by grants R01 AG11622, R01 AG19731, R37 AG002163, and T32 AG00029, from the National Institute on Aging. We are grateful for assistance from Susanne Harris, Leslie Crandell Dawes, and Sara Moore.

References

1. Bar M. A cortical mechanism for triggering top-down facilitation in visual object recognition. *J Cogn Neurosci* 2003;15(4):600–9. [PubMed: 12803970]
2. Bartzokis G, Sultzer D, Lu PH, Nuechterlein KH, Mintz J, Cummings JL. Heterogeneous age-related breakdown of white matter structural integrity: implications for cortical “disconnection” in aging and Alzheimer’s disease. *Neurobiol Aging* 2004;25(7):843–51. [PubMed: 15212838]
3. Basser PJ, Pierpaoli C. A simplified method to measure the diffusion tensor from seven MR images. *Magn Reson Med* 1998;39(6):928–34. [PubMed: 9621916]
4. Beaulieu C. The basis of anisotropic water diffusion in the nervous system—a technical review. *NMR Biomed* 2002;15(7–8):435–55. [PubMed: 12489094]
5. Beck, AT. The Beck depression inventory. New York: Psychological Corporation; 1978.
6. Bruce CJ, Goldberg ME, Bushnell MC, Stanton GB. Primate frontal eye fields. II. Physiological and anatomical correlates of electrically evoked eye movements. *J Neurophysiol* 1985;54(3):714–34. [PubMed: 4045546]
7. Buckner RL, Snyder AZ, Sanders AL, Raichle ME, Morris JC. Functional brain imaging of young, nondemented, and demented older adults. *J Cogn Neurosci* 2000;12(Suppl 2):24–34. [PubMed: 11506645]
8. Cabeza R, Daselaar SM, Dolcos F, Prince SE, Budde M, Nyberg L. Task-independent and task-specific age effects on brain activity during working memory, visual attention and episodic retrieval. *Cereb Cortex* 2004;14(4):364–75. [PubMed: 15028641]
9. Cabeza, R.; Nyberg, L.; Park, D., editors. *Cognitive neuroscience of aging: linking cognitive and cerebral aging*. New York: Oxford University Press; 2005.
10. Caviness VS, Meyer J, Makris N, Kennedy D. MRI-based topographic parcellation of human neocortex: an anatomically specified method with estimate of reliability. *J Cogn Neurosci* 1996;8(6):566–87.
11. Corbetta M, Akbudak E, Conturo TE, Snyder AZ, Ollinger JM, Drury HA, et al. A common network of functional areas for attention and eye movements. *Neuron* 1998;21(4):761–73. [PubMed: 9808463]
12. Corbetta M, Kincade JM, Ollinger JM, McAvoy MP, Shulman GL. Voluntary orienting is dissociated from target detection in human posterior parietal cortex. *Nat Neurosci* 2000;3(3):292–7. [PubMed: 10700263]
13. Corbetta M, Shulman GL. Control of goal-directed and stimulus-driven attention in the brain. *Nat Rev Neurosci* 2002;3(3):201–15. [PubMed: 11994752]
14. de Fockert J, Rees G, Frith C, Lavie N. Neural correlates of attentional capture in visual search. *J Cogn Neurosci* 2004;16(5):751–9. [PubMed: 15200703]
15. Duvernoy, HM. *The human brain: surface, three-dimensional sectional anatomy with MRI, and blood supply*. 2. New York: Springer-Verlag; 1999.
16. Folk CL, Lincourt AE. The effects of age on guided conjunction search. *Exp Aging Res* 1996;22(1):99–118. [PubMed: 8665990]

17. Folstein MF, Folstein SE, McHugh PR. "Mini-mental state". A practical method for grading the cognitive state of patients for the clinician. *J Psychiatr Res* 1975;12(3):189–98. [PubMed: 1202204]
18. Gitelman DR, Nobre AC, Parrish TB, LaBar KS, Kim YH, Meyer JR, et al. A large-scale distributed network for covert spatial attention: further anatomical delineation based on stringent behavioural and cognitive controls. *Brain* 1999;122(Pt 6):1093–106. [PubMed: 10356062]
19. Gitelman DR, Parrish TB, LaBar KS, Mesulam MM. Real-time monitoring of eye movements using infrared video-oculography during functional magnetic resonance imaging of the frontal eye fields. *Neuroimage* 2000;11(1):58–65. [PubMed: 10686117]
20. Grady CL. Functional brain imaging and age-related changes in cognition. *Biol Psychol* 2000;54(1–3):259–81. [PubMed: 11035226]
21. Grady CL, Maisog JM, Horwitz B, Ungerleider LG, Mentis MJ, Salerno JA, et al. Age-related changes in cortical blood flow activation during visual processing of faces and location. *J Neurosci* 1994;14(3 Pt 2):1450–62. [PubMed: 8126548]
22. Greenwood PM. The frontal aging hypothesis evaluated. *J Int Neuropsychol Soc* 2000;6(6):705–26. [PubMed: 11011517]
23. Grosbras MH, Laird AR, Paus T. Cortical regions involved in eye movements, shifts of attention, and gaze perception. *Hum Brain Mapp* 2005;25(1):140–54. [PubMed: 15846814]
24. Head D, Buckner RL, Shimony JS, Williams LE, Akbudak E, Conturo TE, et al. Differential vulnerability of anterior white matter in nondemented aging with minimal acceleration in dementia of the Alzheimer type: evidence from diffusion tensor imaging. *Cereb Cortex* 2004;14(4):410–23. [PubMed: 15028645]
25. Huettel SA, McCarthy G. The effects of single-trial averaging upon the spatial extent of fMRI activation. *Neuroreport* 2001;12(11):2411–6. [PubMed: 11496120]
26. Huettel SA, Misiurek J, Jurkowski AJ, McCarthy G. Dynamic and strategic aspects of executive processing. *Brain Res* 2004;1000(1–2):78–84. [PubMed: 15053955]
27. Jha AP, McCarthy G. The influence of memory load upon delay-interval activity in a working-memory task: an event-related functional MRI study. *J Cogn Neurosci* 2000;12(Suppl 2):90–105. [PubMed: 11506650]
28. Kastner S, Ungerleider LG. Mechanisms of visual attention in the human cortex. *Annu Rev Neurosci* 2000;23:315–41. [PubMed: 10845067]
29. Koyama M, Hasegawa I, Osada T, Adachi Y, Nakahara K, Miyashita Y. Functional magnetic resonance imaging of macaque monkeys performing visually guided saccade tasks: comparison of cortical eye fields with humans. *Neuron* 2004;41(5):795–807. [PubMed: 15003178]
30. Kramer AF, Hahn S, Irwin DE, Theeuwes J. Attentional capture and aging: implications for visual search performance and oculomotor control. *Psychol Aging* 1999;14(1):135–54. [PubMed: 10224638]
31. LaBerge, D. Networks of attention. In: Gazzaniga, MS., editor. *The new cognitive neurosciences*. 2. Cambridge, MA: MIT Press; 2000. p. 711–23.
32. Le Bihan D. Looking into the functional architecture of the brain with diffusion MRI. *Nat Rev Neurosci* 2003;4(6):469–80. [PubMed: 12778119]
33. Leichnetz GR, Goldberg ME. Higher centers concerned with eye movement and visual attention: cerebral cortex and thalamus. *Rev Oculomot Res* 1988;2:365–429. [PubMed: 3153653]
34. Leonards U, Sunaert S, Van Hecke P, Orban GA. Attention mechanisms in visual search—an fMRI study. *J Cogn Neurosci* 2000;12(Suppl 2):61–75. [PubMed: 11506648]
35. Luna B, Thulborn KR, Strojwas MH, McCurtain BJ, Berman RA, Genovese CR, et al. Dorsal cortical regions subserving visually guided saccades in humans: an fMRI study. *Cereb Cortex* 1998;8(1):40–7. [PubMed: 9510384]
36. Madden DJ, Turkington TG, Provenzale JM, Denny LL, Langley LK, Hawk TC, et al. Aging and attentional guidance during visual search: functional neuroanatomy by positron emission tomography. *Psychol Aging* 2002;17(1):24–43. [PubMed: 11931285]
37. Madden DJ, Turkington TG, Provenzale JM, Hawk TC, Hoffman JM, Coleman RE. Selective and divided visual attention: age-related changes in regional cerebral blood flow measured by H₂ 15O PET. *Hum Brain Mapp* 1997;5(6):389–409.

38. Madden, DJ.; Whiting, WL. Age-related changes in visual attention. In: Costa, PT.; Siegler, IC., editors. *Recent advances in psychology and aging*. Amsterdam: Elsevier; 2004. p. 41-88.
39. Madden DJ, Whiting WL, Cabeza R, Huettel SA. Age-related preservation of top-down attentional guidance during visual search. *Psychol Aging* 2004;19(2):304–9. [PubMed: 15222823]
40. Madden, DJ.; Whiting, WL.; Huettel, SA. Age-related changes in neural activity during visual perception and attention. In: Cabeza, R.; Nyberg, L.; Park, D., editors. *Cognitive neuroscience of aging: linking cognitive and cerebral aging*. New York: Oxford University Press; 2005. p. 157-85.
41. Madden DJ, Whiting WL, Huettel SA, White LE, MacFall JR, Provenzale JM. Diffusion tensor imaging of adult age differences in cerebral white matter: relation to response time. *Neuroimage* 2004;21(3):1174–81. [PubMed: 15006684]
42. Madden DJ, Whiting WL, Provenzale JM, Huettel SA. Age-related changes in neural activity during visual target detection measured by fMRI. *Cereb Cortex* 2004;14(2):143–55. [PubMed: 14704211]
43. Madden DJ, Whiting WL, Spaniol J, Bucur B. Adult age differences in the implicit and explicit components of top-down attentional guidance during visual search. *Psychol Aging* 2005;20(2):317–29. [PubMed: 16029095]
44. McDowd, JM.; Shaw, RJ. Attention and aging: a functional perspective. In: Craik, FIM.; Salthouse, TA., editors. *The handbook of aging and cognition*. 2. Hillsdale, NJ: Erlbaum; 2000. p. 221-92.
45. Milham MP, Erickson KI, Banich MT, Kramer AF, Webb A, Wszalek T, et al. Attentional control in the aging brain: insights from an fMRI study of the Stroop task. *Brain Cogn* 2002;49(3):277–96. [PubMed: 12139955]
46. Moseley M. Diffusion tensor imaging and aging—a review. *NMR Biomed* 2002;15(7–8):553–60. [PubMed: 12489101]
47. Moseley M, Bammer R, Illes J. Diffusion-tensor imaging of cognitive performance. *Brain Cogn* 2002;50(3):396–413. [PubMed: 12480486]
48. Nielson KA, Langenecker SA, Garavan H. Differences in the functional neuroanatomy of inhibitory control across the adult life span. *Psychol Aging* 2002;17(1):56–71. [PubMed: 11931287]
49. Nieto-Castanon A, Ghosh SS, Tourville JA, Guenther FH. Region of interest based analysis of functional imaging data. *Neuroimage* 2003;19(4):1303–16. [PubMed: 12948689]
50. Nobre AC, Gitelman DR, Dias EC, Mesulam MM. Covert visual spatial orienting and saccades: overlapping neural systems. *Neuroimage* 2000;11(3):210–6. [PubMed: 10694463]
51. O’Sullivan M, Jones DK, Summers PE, Morris RG, Williams SC, Markus HS. Evidence for cortical “disconnection” as a mechanism of age-related cognitive decline. *Neurology* 2001;57(4):632–8. [PubMed: 11524471]
52. Peters A, Sethares C. Aging and the myelinated fibers in pre-frontal cortex and corpus callosum of the monkey. *J Comp Neurol* 2002;442(3):277–91. [PubMed: 11774342]
53. Petrides, M.; Pandya, DN. Association pathways of the prefrontal cortex and functional observations. In: Stuss, DT.; Knight, RT., editors. *Principles of frontal lobe function*. New York: Oxford University Press; 2002. p. 31-50.
54. Pfefferbaum A, Adalsteinsson E, Sullivan EV. Frontal circuitry degradation marks healthy adult aging: evidence from diffusion tensor imaging. *Neuroimage* 2005;26(3):891–9. [PubMed: 15955499]
55. Pfefferbaum A, Sullivan EV, Hedehus M, Lim KO, Adalsteinsson E, Moseley M. Age-related decline in brain white matter anisotropy measured with spatially corrected echo-planar diffusion tensor imaging. *Magn Reson Med* 2000;44(2):259–68. [PubMed: 10918325]
56. Pollmann S, Weidner R, Humphreys GW, Olivers CN, Muller K, Lohmann G, et al. Separating distractor rejection and target detection in posterior parietal cortex—an event-related fMRI study of visual marking. *Neuroimage* 2003;18(2):310–23. [PubMed: 12595185]
57. Quinlan PT. Visual feature integration theory: past, present, and future. *Psychol Bull* 2003;129(5):643–73. [PubMed: 12956538]
58. Raz, N. Aging of the brain and its impact on cognitive performance: integration of structural and functional findings. In: Craik, FIM.; Salt-house, TA., editors. *Handbook of aging and cognition*. 2. Mahwah, NJ: Erlbaum; 2000. p. 1-90.

59. Rosano C, Krisky CM, Welling JS, Eddy WF, Luna B, Thulborn KR, et al. Pursuit and saccadic eye movement subregions in human frontal eye field: a high-resolution fMRI investigation. *Cereb Cortex* 2002;12(2):107–15. [PubMed: 11739259]
60. Rosler A, Mapstone ME, Hays AK, Mesulam MM, Rademaker A, Gitelman DR, et al. Alterations of visual search strategy in Alzheimer's disease and aging. *Neuropsychology* 2000;14(3):398–408. [PubMed: 10928743]
61. Rubin DC. Frontal–striatal circuits in cognitive aging: evidence for caudate involvement. *Aging Neuropsychol Cogn* 1999;6(4):241–59.
62. Salat DH, Tuch DS, Greve DN, van der Kouwe AJ, Hevelone ND, Zaleta AK, et al. Age-related alterations in white matter microstructure measured by diffusion tensor imaging. *Neurobiol Aging* 2005;26(8):1215–27. [PubMed: 15917106]
63. Salthouse TA. The processing-speed theory of adult age differences in cognition. *Psychol Rev* 1996;103(3):403–28. [PubMed: 8759042]
64. Salthouse TA. What do adult age differences in the Digit Symbol Substitution Test reflect? *J Gerontol* 1992;47(3):P121–8. [PubMed: 1573192]
65. Sandell JH, Peters A. Effects of age on nerve fibers in the rhesus monkey optic nerve. *J Comp Neurol* 2001;429(4):541–53. [PubMed: 11135234]
66. Schneider, BA.; Pichora-Fuller, MK. Implication of perceptual deterioration for cognitive aging research. In: Craik, FIM.; Salthouse, TA., editors. *The handbook of aging and cognition*. 2. Mahwah, NJ: Erlbaum; 2000. p. 155-219.
67. Shulman GL, Corbetta M, Buckner RL, Raichle ME, Fiez JA, Miezin FM, et al. Top-down modulation of early sensory cortex. *Cereb Cortex* 1997;7(3):193–206. [PubMed: 9143441]
68. Spear PD. Neural bases of visual deficits during aging. *Vision Res* 1993;33(18):2589–609. [PubMed: 8296455]
69. Tabachnick, BG.; Fidell, LS. *Using multivariate statistics*. 4. Needham Heights, MA: Allyn and Bacon; 2001.
70. Tisserand DJ, Jolles J. On the involvement of prefrontal networks in cognitive ageing. *Cortex* 2003;39(4–5):1107–28. [PubMed: 14584569]
71. Verhaeghen P, Cerella J. Aging, executive control, and attention: a review of meta-analyses. *Neurosci Biobehav Rev* 2002;26(7):849–57. [PubMed: 12470697]
72. Visscher KM, Miezin FM, Kelly JE, Buckner RL, Donaldson DI, McAvoy MP, et al. Mixed blocked/event-related designs separate transient and sustained activity in fMRI. *Neuroimage* 2003;19(4):1694–708. [PubMed: 12948724]
73. Watson DG, Maylor EA. Aging and visual marking: selective deficits for moving stimuli. *Psychol Aging* 2002;17(2):321–39. [PubMed: 12061415]
74. Wechsler, D. *Wechsler adult intelligence scale—revised*. New York: Psychological Corporation; 1981.
75. Wecker NS, Kramer JH, Wisniewski A, Delis DC, Kaplan E. Age effects on executive ability. *Neuropsychology* 2000;14(3):409–14. [PubMed: 10928744]
76. West RL. An application of prefrontal cortex function theory to cognitive aging. *Psychol Bull* 1996;120(2):272–92. [PubMed: 8831298]
77. Woldorff MG, Hazlett CJ, Fichtenholtz HM, Weissman DH, Dale AM, Song AW. Functional parcellation of attentional control regions of the brain. *J Cogn Neurosci* 2004;16(1):149–65. [PubMed: 15006044]
78. Wolfe, JM. Visual search. In: Pashler, H., editor. *Attention*. East Sussex, UK: Psychology Press; 1998. p. 13-73.
79. Yantis S, Schwarzbach J, Serences JT, Carlson RL, Steinmetz MA, Pekar JJ, et al. Transient neural activity in human parietal cortex during spatial attention shifts. *Nat Neurosci* 2002;5(10):995–1002. [PubMed: 12219097]

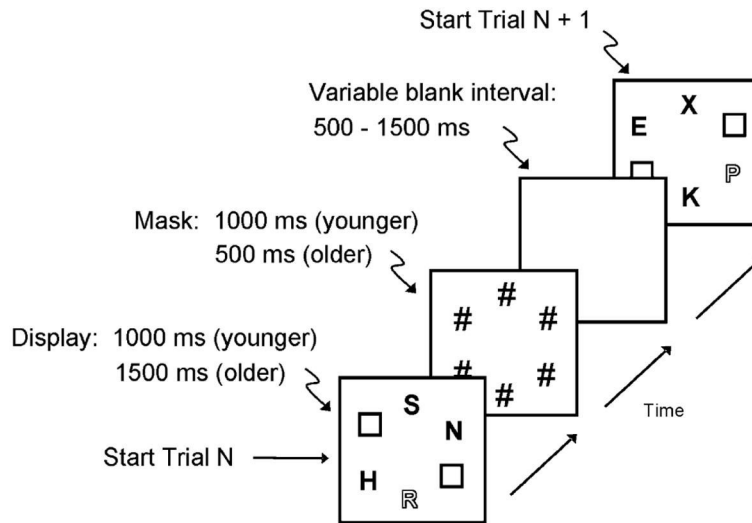


Fig 1.

Sequence of events on individual trials in the visual search task. On each trial, participants viewed a display containing three gray letters and one red letter (a color singleton). Participants made a two-choice response regarding which one of two targets (E and R) was present in the display. The singleton is represented in the figure by the outline font. Within each block of trials (varied across scanner runs) the probability that the singleton was the target was either low (25%; neutral condition) or high (75%; guided condition).

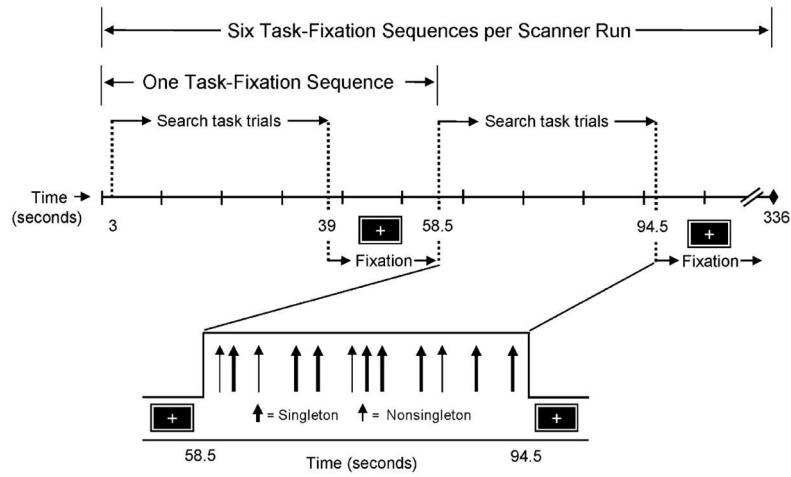
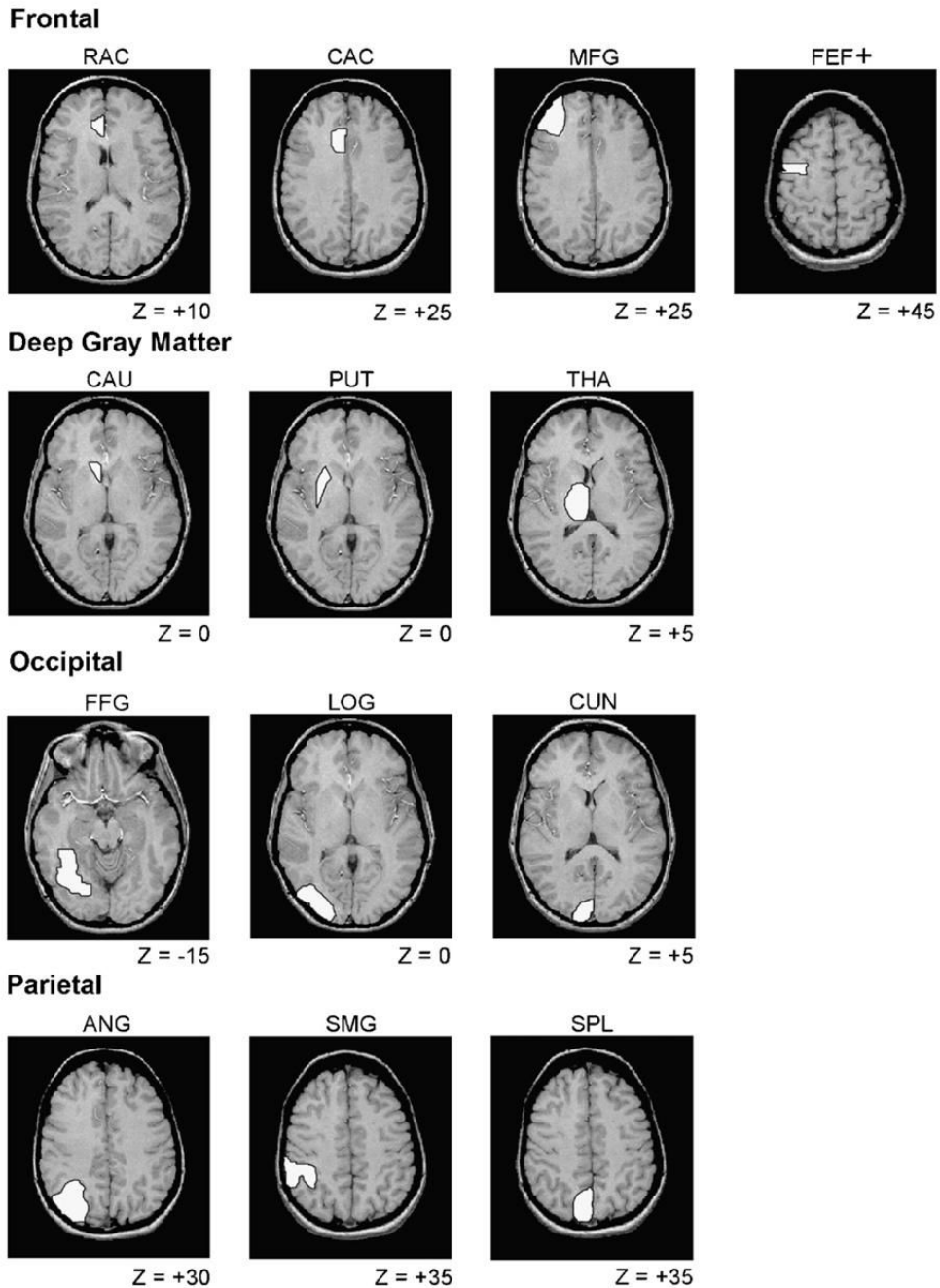


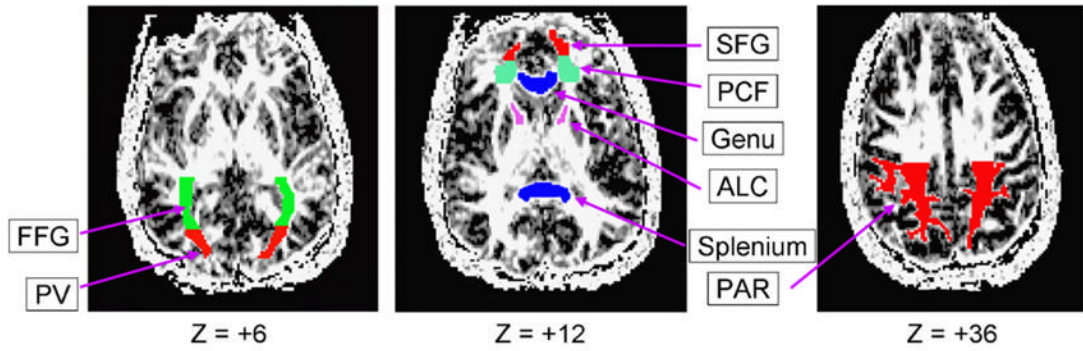
Fig 2.

fMRI event-related design. Each scanner run comprised either neutral or guided condition trials. The run contained 72 visual search trials: 6 task-fixation sequences, with each set of 12 task trials (36 s) followed by a 19.5 s fixation period. The figure illustrates a guided condition run; locations of individual trials in the task period are represented by arrows. The interval between individual trials was jittered to increase the temporal resolution of the estimated HDR.

**Fig 3.**

Examples of gray matter ROIs. For each ROI, an example is displayed of one representative T₁-weighted MR slice, with Z value (in mm) for location of this slice relative to the AC-PC plane. Only the left hemisphere ROIs are illustrated, but all ROIs were drawn in both hemispheres. Although only one slice is illustrated, each ROI could include multiple slices (see Table 1), and the ROIs were defined for each participant individually. RAC, rostral portion of anterior cingulate; CAC, caudal portion of anterior cingulate; FEF+, frontal eye field; MFG, middle frontal gyrus; CAU, caudate; PUT, putamen; THA, thalamus; CUN, cuneus; FFG, fusiform gyrus; LOG, lateral occipital gyri; ANG, angular gyrus; SMG, supramarginal gyrus;

SPL, superior parietal lobule. We use the label FEF+ to distinguish our ROI in BA 6 from the frontal eye field defined classically in BA 8 [29].

**Fig 4.**

Examples of white matter ROIs. The ROIs were drawn on diffusion tensor images set at a lower maximum image intensity. Although only one image slice is illustrated, each ROI could include multiple slices (see Table 2), and the ROIs were defined for each participant individually. Z, millimeters above the AC–PC plane; FFG, fusiform gyrus; PV, posterior visual region; SFG, superior frontal gyrus; PCF, pericallosal frontal region; genu, genu of corpus callosum; ALC, anterior limb of internal capsule; splenium, splenium of corpus callosum; PAR, parietal.

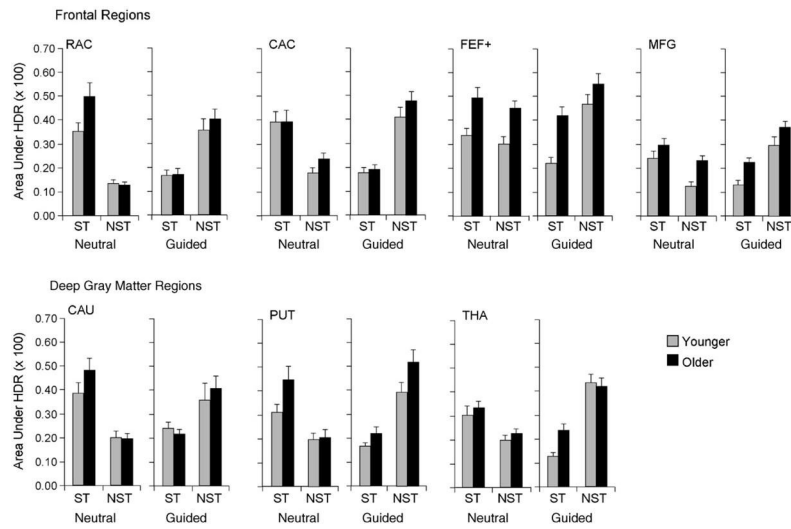


Fig 5. Magnitude of event-related fMRI activation for frontal and deep gray matter ROIs. Activation is defined by area under the HDR curve associated with individual trials, as a function of age group (younger, older), task condition (neutral, guided), target type (singleton, nonsingleton), and ROI. Data are presented as means, averaged over left and right hemisphere; error bars represent 1 S.E.; ST, singleton target; NST, nonsingleton target. See Fig. 3 legend for ROI labels.

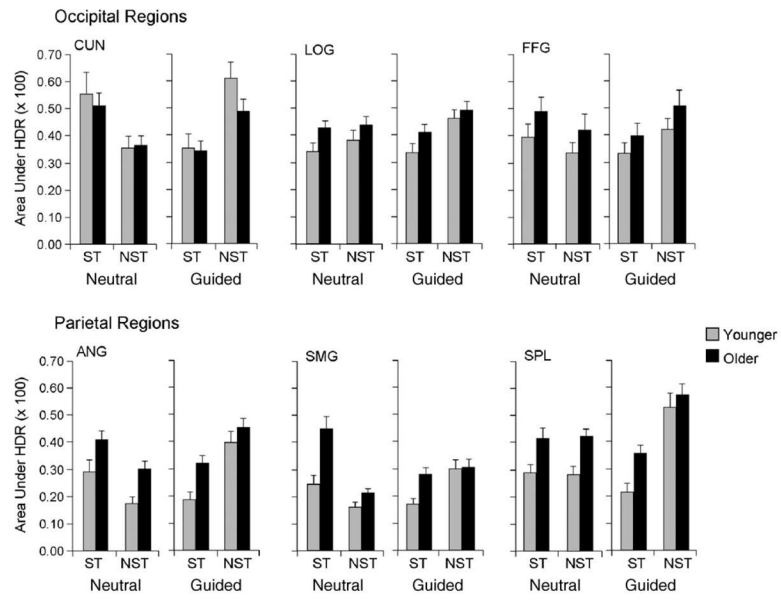


Fig 6. Magnitude of event-related fMRI activation for occipital and parietal ROIs, as described in Fig. 5 legend.

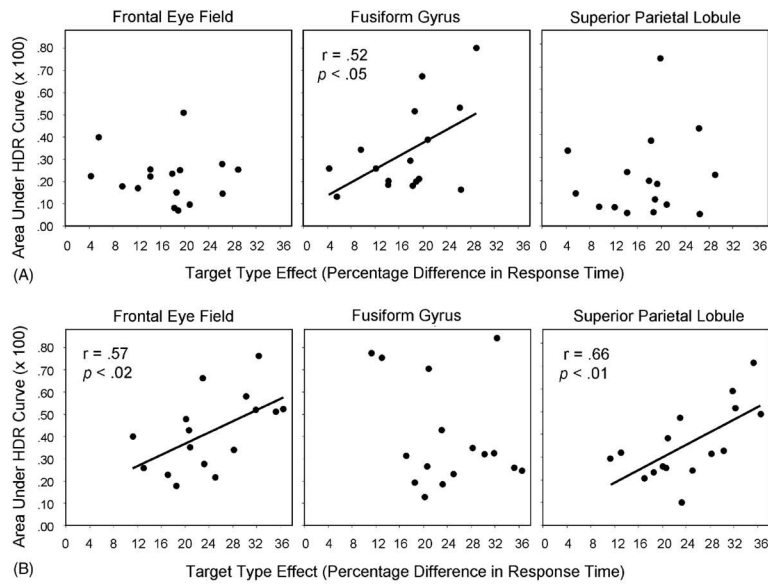


Fig 7. Correlation between fMRI activation (area under the HDR curve) in guided condition and search performance (target type effect: percentage difference in response time to singleton and nonsingleton targets). (A) For younger adults, the correlation was significant only for the fusiform gyrus. (B) For older adults, the correlation was significant only for the frontal eye field and superior parietal lobule.

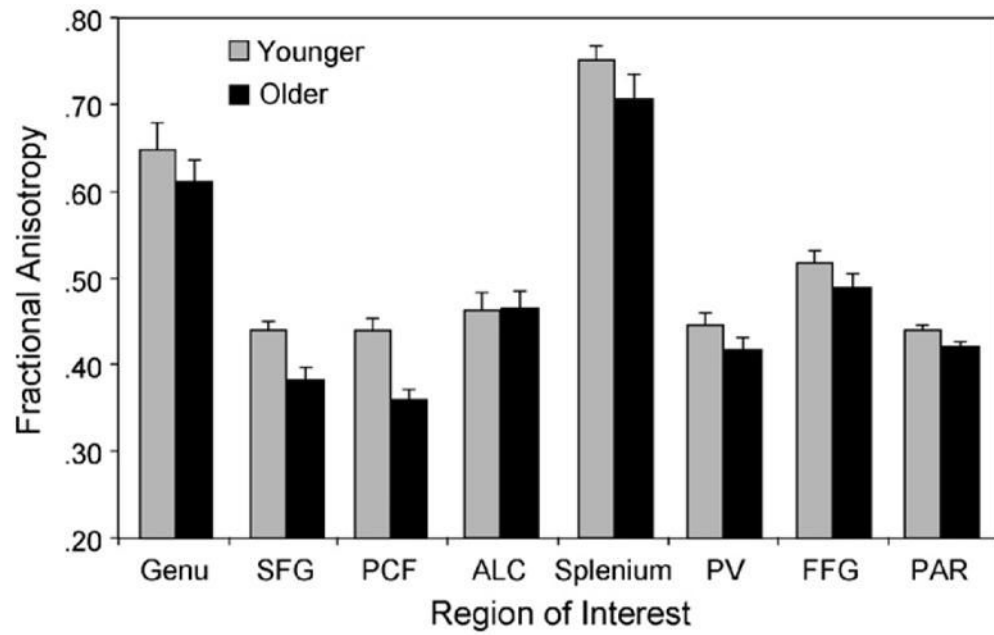


Fig 8. Mean FA as a function of age group and ROI. Data are presented as means, averaged over left and right hemisphere; error bars represent 1S.E. See Fig. 4 legend for ROI labels.

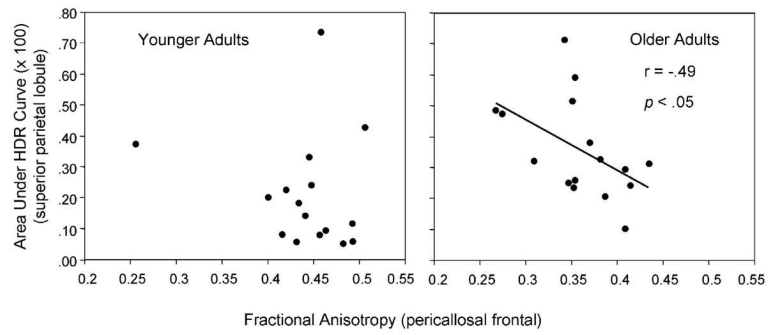


Fig 9. Correlation between fMRI activation (area under the HDR curve) in guided condition (singleton target trials) for the superior parietal lobule gray matter ROI and pericallosal frontal FA. Increasing activation was associated with lower FA for older adults but not for younger adults.

Table 1

Gray matter regions of interest

ROI	Max. slice	BA	Region size (voxels)	
			Younger adults	Older adults
Frontal				
RAC	5	24/32	92 (29)	104 (33)
CAC	2	24/32	76 (25)	61 (18)
FEF+	4	6	102 (20)	111 (22)
MFG	11	8/9/10/46	907 (159)	834 (125)
Deep gray matter				
CAU	4	–	58 (18)	48 (9)
PUT	3	–	90 (28)	65 (21)
THA	3	–	163 (46)	157 (37)
Occipital				
CUN	9	17/18/19	343 (107)	365 (75)
LOG	6	18/19	499 (119)	530 (106)
FFG	2	36/37	170 (49)	177 (74)
Parietal				
ANG	6	39	461 (105)	440 (123)
SMG	7	40	495 (112)	458 (134)
SPL	8	7	463 (111)	463 (99)

Note: Imaging slices were near-axial oblique, 5 mm thick, parallel to AC–PC. ROI, region of interest. Max. slice, maximum number of slices included in ROI. BA, Brodmann areas included in ROI. Region size is mean number of voxels across participants; standard deviations are in parentheses. See Fig. 3 legend for ROI labels.

Table 2

White matter regions of interest

ROI	Max. slice	Region size (voxels)	
		Younger adults	Older adults
Genu *	4	107 (38)	83 (26)
Splenium	4	110 (53)	118 (58)
SFG *	3	195 (69)	122 (44)
PCF *	3	239 (81)	173 (53)
ALC	3	65 (15)	62 (21)
PV	4	284 (80)	243 (72)
FFG *	3	253 (73)	275 (88)
PAR *	3	1132 (265)	873 (289)

Note: Imaging slices were near-axial oblique, 6 mm thick, parallel to AC–PC. Max. slice, maximum number of slices included in ROI. ROI, region of interest. Region size is mean number of voxels across participants; standard deviations are in parentheses. See Fig. 4 legend for ROI labels.

* Age group difference in region size significant at $p < 0.05$.

Table 3
Performance in visual search task as a function of age group, task condition, and target type

Condition	Response time		Error rate	
	Younger adults	Older adults	Younger adults	Older adults
Neutral				
Singleton targets	627 (40)	819 (111)	2.08 (4.11)	1.74 (2.48)
Nonsingleton targets	668 (60)	863 (107)	1.77 (2.10)	1.12 (1.34)
Guided				
Singleton targets	595 (32)	734 (87)	1.35 (1.45)	0.42 (0.67)
Nonsingleton targets	725 (77)	975 (127)	2.31 (3.21)	1.04 (2.24)

Note: Response times are means (across participants) of median values, in ms, for correct responses. Error rate values are mean percentages of incorrect responses. Standard deviations are in parentheses.

Table 4

Significant *F* values in analysis of variance of magnitude of fMRI activation

	Multivariate effects	Univariate effects	
Frontal ROIs			
Age group		RAC	MFG
Condition × target type	4.35**	—	17.89***
Deep gray matter ROIs	23.30***	88.73***	10.25**
Target type	3.61*	CAU	THA
Condition × target type	23.14***	—	7.85**
Occipital ROIs		25.14***	35.33***
Condition × target type	7.73**	CUN***	FFG
Parietal ROIs		20.85***	4.11*
Age group		ANG	SPL**
Condition	4.57**	12.11**	9.53**
Parietal ROIs	3.43*	4.12*	6.23*
Target type		ANG	SPL**
Condition × target type	9.59**	—	15.53***
	5.72**	15.23***	12.06**
		—	16.09***

Note: Values are *F* ratio. For frontal ROIs, multivariate d.f. = 4, 27; for deep gray matter, occipital, and parietal ROIs, multivariate d.f. = 3, 28; for all ROIs, univariate d.f. = 1, 30. Multivariate analyses included data from each ROI as a separate dependent variable. In both the multivariate and univariate analyses, the independent variables were age group (younger vs. older), and task condition (guided vs. neutral). Only correct-response trials were included in the analyses. The dependent variable representing the magnitude of fMRI activation was the area under the HDR curve associated with an average task trial sequence. ROI, region of interest. See Fig. 3 legend for ROI labels.

* $p < 0.05$.

** $p < 0.01$.

*** $p < 0.001$.